

Thermolysis of *tert*-Butyl Phenylperacetates: Delicate Control of the Rates through Contributions from Translational and Rotational Entropy[†]

Sung Soo Kim,* In Sang Baek, Alexey Tuchkin,[‡] and Kyoung Moon Go

Department of Chemistry and Center for Chemical Dynamics, Inha University,
Inchon 402-751, South Korea

sungsoo@inha.ac.kr

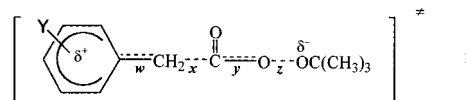
Received February 6, 2001

The first-order rate constants (k_Y) at several temperatures in CDCl_3 were measured for thermal decompositions of $\text{YC}_6\text{H}_4\text{CH}_2\text{CO}_3\text{C}(\text{CH}_3)_3$ with Y being *p*-OCH₃, *p*-OPh, *p*-CH₃, *p*-Ph, *p*-H, *p*-Cl, *m*-Cl, and *p*-NO₂. The relative rates (k_Y/k_H) exhibit excellent ρ^+/σ^+ Hammett correlations with $\rho^+ < 0$, indicating a polar TS. Activation parameters (ΔH^\ddagger_Y and ΔS^\ddagger_Y) and their differential terms ($\Delta\Delta H^\ddagger_{Y-H}$ and $\Delta\Delta S^\ddagger_{Y-H}$) were obtained from the Eyring plot. Differential activation terms ($\Delta\Delta H^\ddagger_{Y-H}$ and $\Delta\Delta S^\ddagger_{Y-H}$) disclose an isokinetic relation with *p*-CH₃, *p*-Ph, *p*-H, *p*-Cl, and *m*-Cl (isokinetic temp, 230 K). However, *p*-OCH₃ and *p*-OPh show negative deviations, and a positive deviation occurs with *p*-NO₂. Plot of $\Delta\Delta H^\ddagger_{Y-H}$ vs σ^+ exhibits a good linear relation ($r = 0.95$) with a slope ($\alpha_1 = -3.34$). A better linear correlation ($r = 0.97$) and steeper slope ($\alpha_2 = -5.22$) were observed for $\Delta\Delta S^\ddagger_{Y-H}$ vs σ^+ . Negatively larger slope ($\alpha_2 = -5.22$) may point to entropy control of rates. Differential activation parameters ($\Delta\Delta H^\ddagger_{Y-H}$ and $\Delta\Delta S^\ddagger_{Y-H}$) reflect variations of activation process. Differential activation entropies ($\Delta\Delta S^\ddagger_{Y-H}$) are discussed in terms of contributions of translational and rotational entropies. Similar deviation behaviors of *p*-OCH₃, *p*-OPh, and *p*-NO₂ were again observed for the both plots. *p*-NO₂ can strongly destabilize the cationic site of the polar TS but serves an eminent spin delocalizer for the *homolytic* TS.

Introduction

Thermal decompositions of *tert*-butyl phenylperacetates^{1–7} occur through simultaneous two-bond scissions to yield a carbon dioxide, benzyl and *tert*-butoxy radical. Both activation enthalpy (ΔH^\ddagger) and activation entropy (ΔS^\ddagger) gradually decrease¹ when R in $\text{RCO}_3\text{C}(\text{CH}_3)_3$ is varied in the order of C_6H_5 ($\Delta H^\ddagger = 33.5 \text{ kcal mol}^{-1}$, $\Delta S^\ddagger = 7.8 \text{ eu}$), $\text{C}_6\text{H}_5\text{CH}_2$ ($\Delta H^\ddagger = 28.7 \text{ kcal mol}^{-1}$, $\Delta S^\ddagger = 3.9 \text{ eu}$),⁸ $(\text{C}_6\text{H}_5)_2\text{CH}$ ($\Delta H^\ddagger = 24.3 \text{ kcal mol}^{-1}$, $\Delta S^\ddagger = -1.0 \text{ eu}$),⁸ $\text{C}_6\text{H}_5\text{CH}=\text{CH}-\text{CH}_2$ ($\Delta H^\ddagger = 23.5 \text{ kcal mol}^{-1}$, $\Delta S^\ddagger = -5.9 \text{ eu}$).⁸ The synchronization of the bond cleavages² produces remarkably small activation volumes ($\Delta V^\ddagger = 1\text{--}3 \text{ cm}^3 \text{ mol}^{-1}$). Accordingly, decrease of the activation parameters (ΔH^\ddagger , ΔS^\ddagger , ΔV^\ddagger) has been recently⁷ explained in terms of formation of π -bonds *w* and *y* in **1**. Viscosity studies of the solvents⁴ have introduced a method to

distinguish the mechanism between one-bond (*z*) and two-bond (*x* and *z*) homolyses. In the previous work,⁷ extent of rupture of bond *x* is shown to be seriously influenced by substituents, which provokes significant variations of secondary α -deuterium kinetic isotope effects.



Hydrogen atom abstractions from substituted toluenes⁹ and cumenes¹¹ and β -scissions of the carbinyl oxy radicals¹⁰ reveal entropy control of rates via the polar substituent interactions. Only relative rates were available with previous studies^{9–11} thereby providing differential activation terms ($\Delta\Delta H^\ddagger_{Y-H}$ and $\Delta\Delta S^\ddagger_{Y-H}$) derived from the Eyring equation.¹² The positive sign of differential activation entropies ($\Delta\Delta S^\ddagger_{Y-H}$)^{9–11} with electron-donating substituents is ascribed to the dominance of the

[†] The late Professor Glen A. Russell has been a *Distinguished Foreign Adviser* for this investigation. We are heavily indebted to his mentorship.

[‡] A visiting scholar from St. Petersburg State University by a grant from the Science Technology Policy Institute under the Korea-Russia manpower exchange program (1996).

(1) (a) Bartlett, P. D.; Hiatt, R. R. *J. Am. Chem. Soc.* **1958**, *80*, 1398. (b) Bartlett, P. D.; Simons, D. M. *J. Am. Chem. Soc.* **1960**, *82*, 1753. (c) Bartlett, P. D.; Rüchardt, C. *J. Am. Chem. Soc.* **1960**, *82*, 1756.

(2) (a) Neuman, R. C., Jr.; Behar, J. V. *J. Am. Chem. Soc.* **1967**, *89*, 4549. (b) Neuman, R. C., Jr.; Behar, J. V. *J. Am. Chem. Soc.* **1969**, *91*, 6024. (c) Neuman, R. C., Jr.; Behar, J. V. *J. Org. Chem.* **1971**, *36*, 654. (d) Neuman, R. C., Jr.; Behar, J. V. *J. Org. Chem.* **1971**, *36*, 657.

(3) (a) Koenig, T.; Wolf, R. *J. Am. Chem. Soc.* **1969**, *91*, 2574. (b) Koenig, T.; Huntington, J.; Cruthoff, R. *J. Am. Chem. Soc.* **1970**, *92*, 5413.

(4) Pryor, W. A.; Smith, K. *J. Am. Chem. Soc.* **1970**, *92*, 5403.

(5) Pryor, W. A.; Smith, K. *Int. J. Chem. Kinet.* **1971**, *3*, 387.

(6) Wolf, R. A.; Trocino, R. J.; Rozich, W. R.; Sabeta, I. C.; Ordway, R. J., Jr. *J. Org. Chem.* **1998**, *63*, 3814.

(7) Kim, S. S.; Tuchkin, A. *J. Org. Chem.* **1999**, *64*, 3821.

(8) The rates are accelerated by 65 times at 60 °C when R = $(\text{C}_6\text{H}_5)_2\text{CH}$ takes the place of R = $\text{C}_6\text{H}_5\text{CH}_2$ in the decomposition of $\text{RCO}_3\text{C}(\text{CH}_3)_3$. The skeletal variation of R causes a relatively large change of activation enthalpy ($\Delta\Delta H^\ddagger = 24.3 - 28.7 = -4.4 \text{ kcal mol}^{-1}$) that may well outweigh the entropy decrease ($-1 - 3.9 = -4.9 \text{ eu}$) to achieve enthalpy control of rates. The negative values of ΔS^\ddagger are shown with R being $(\text{C}_6\text{H}_5)_2\text{CH}$ and $\text{C}_6\text{H}_5\text{CH}=\text{CH}-\text{CH}_2$. Extensive charge delocalizations occurring in $(\text{C}_6\text{H}_5)_2\text{CH}^{\bullet+}$ and $\text{C}_6\text{H}_5\text{CH}=\text{CH}-\text{CH}_2^{\bullet+}$ of the corresponding TS can prohibit the free rotation of phenyl rings. The negative figures ($\Delta S^\ddagger < 0$) should be due to reduction of the rotational entropy.

(9) Kim, S. S.; Choi, S. Y.; Kang, C. H. *J. Am. Chem. Soc.* **1985**, *107*, 4234.

(10) Kim, S. S.; Kim, H. R.; Kim, H. B.; Youn, S. J.; Kim, C. J. *J. Am. Chem. Soc.* **1994**, *116*, 2754.

(11) Kim, S. S.; Kim, C. S. *J. Org. Chem.* **1999**, *64*, 9261.

Table 1. Kinetic Data for Thermal Decompositions of *tert*-Butyl Phenylperacetates in CDCl₃

$$\text{YC}_6\text{H}_4\text{CH}_2\overset{\text{O}}{\parallel}\text{COOC}(\text{CH}_3)_3 \longrightarrow \text{YC}_6\text{H}_4\text{CH}_2^\bullet + \text{CO}_2 + (\text{CH}_3)_3\text{CO}^\bullet$$

temp, °C	$k_Y^a \times 10^4, \text{s}^{-1} (k_Y/k_H)$								Hammett correlations ^b	
	<i>p</i> -CH ₃ O	<i>p</i> -PhO	<i>p</i> -CH ₃	<i>p</i> -Ph	H	<i>p</i> -Cl	<i>m</i> -Cl	<i>p</i> -NO ₂	ρ^+ (<i>r</i>)	ρ (<i>r</i>)
60	1.25 (10.7)	0.465 (3.97)	0.26 (2.22)	0.221 (1.89)	0.117 (1.00)	0.101 (0.86)	0.050 ^d (0.43)	0.019 ^d (0.138)	-1.13 (0.996)	-1.53 (0.913)
70	4.05 (11.04)	1.50 (4.09)	0.817 (2.23)	0.745 (2.03)	0.367 (1.00)	0.319 (0.87)	0.151 (0.41)	0.058 ^d (0.158)	-1.15 (0.996)	-1.56 (0.912)
80	11.90 (11.23)	4.82 (4.55)	2.63 (2.48)	2.29 (2.16)	1.06 (1.00)	0.84 (0.79)	0.424 (0.40)	0.165 (0.156)	-1.18 (0.996)	-1.596 (0.911)
80 ^c	9.207 (12.89)	3.04 (4.26)	1.89 (2.65)	1.76 (2.46)	0.714 (1.00)	0.584 (0.818)	0.289 (0.404)	0.128 (0.179)	-1.17 (0.992)	-1.631 (0.905)
90	35.67 (11.7)	13.9 (4.56)	8.36 (2.74)	7.17 (2.35)	3.05 (1.00)	2.79 (0.91)	1.26 (0.41)	0.44 (0.144)	-1.20 (0.997)	-1.642 (0.919)
100	111.8 ^d (11.95)	45.38 ^d (4.85)	24.98 (2.67)	19.54 (2.09)	9.36 (1.00)	7.60 (0.81)	3.61 (0.39)	1.438 (0.154)	-1.21 (0.997)	-1.629 (0.910)
110	333.9 ^d (12.25)	138.2 ^d (5.07)	78.85 ^d (2.89)	72.06 ^d (2.64)	27.27 (1.00)	22.48 (0.82)	9.77 (0.36)	3.855 (0.141)	-1.26 (0.996)	-1.701 (0.912)

^a The values of k_Y were derived from the plot of $\ln C/C_0 = k_Y t$. The linearities of the plot carry correlation coefficient $r \geq 0.9990$ in most cases. Refer to Supporting Information. ^b Hammett substituent constants were taken from ref 14. ^c CCl₄ was used for solvent. ^d The peresters decomposed either too quickly or too slowly at the temperature specified to measure the accurate rates. Therefore, the figures were obtained by the extrapolations utilizing the relative rates.

bond-breaking (*x*) that augments the translational degrees of freedom.¹² The bond cleavage is inevitably accompanied by formation of a π bond (*w*) causing restricted rotations. Increment of translational entropy may well overwhelm^{9–11} diminution of the rotational entropy. Fortunately, homolysis of present peresters allows us to measure the first-order rate constants and corresponding activation parameters (ΔH^\ddagger_Y and ΔS^\ddagger_Y) absolutely. We'd like to herein emphasize that substituents can exert profound influences in controlling the TS structure.

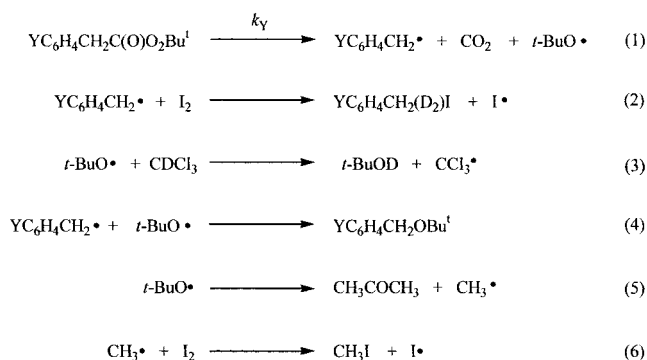
Results and Discussion

Preparation and Thermolysis of the Peresters.

Various ring-substituted *tert*-butyl phenylperacetates **2** were synthesized according to the known methods.^{1,7} Reactions at 80 °C for 5 half-lives in degassed and sealed Pyrex ampules containing **2** (0.05 M), I₂ (0.2–0.4 M), and CH₃CN (0.02 M, internal standard) in CDCl₃ gave rise to benzyl iodide (90.8), *tert*-butyl benzyl ether (4.5), *tert*-butyl alcohol (54.3), methyl iodide (43.3), and acetone (43.3) (Scheme 1). The figures in the parenthesis correspond to mol % of products based on the amount of a perester decomposed. The products were identified by GC–MS and NMR and quantified by NMR. The material balance indicates 95.3% conservation of protons of benzyl moiety of **2**.

Determination of Absolute Rates, Hammett Correlations, and Activation Parameters. The rates of decomposition of **2** in CDCl₃ were obtained at the temperatures by measuring periodically its depletion. The consumption was monitored by disappearance of the proton peak of benzyl ($\delta = 3.6$ –3.7). The rate constants

Scheme 1



(k_Y) were measured with $\ln(C_0/C_t) = k_Y t$. The magnitude of peak of benzylic protons was used for C_0 and C_t . The plots¹³ of $\ln(C_0/C_t)$ vs t revealed excellent linearities with correlation coefficients $r \geq 0.9990$ in most cases thus making it possible to assign reliable values of k_Y . Hammett reaction constants were obtained with σ^+ and σ . The better correlations have been found with ρ^+/σ^+ . The values of ρ^+ become more negative with higher temperatures. These kinetic data are tabulated in Table 1. Activation parameters and their differential terms were obtained from the Eyring plot¹² (Figure 1). Table 2 reveals the activation terms and their differentials. An isokinetic relation is attained with *p*-CH₃, *p*-Ph, *p*-H, *p*-Cl, and *m*-Cl (Figure 2; isokinetic temp T_k , 230 K). Plots of $\Delta\Delta H^\ddagger_{Y-H}$ vs σ^+ and $T\Delta\Delta S^\ddagger_{Y-H}$ vs σ^+ are given in Figures 3 and 4, respectively. *p*-OCH₃ and *p*-OPh persistently show negative deviations, whereas positive deviations occur with *p*-NO₂ for Figures 2, 3, and 4, respectively.

Highlight of the Homolytic Reactions. The concerted bond-breaking yields a polar transition state (TS, **1**) where the positive charge is delocalized into the phenyl ring. Virtually the same values of ρ^+ are obtained with various solvents ($\rho^+ = -1.18$ in CDCl₃, $\rho^+ = -1.17$ in CCl₄, $\rho^+ = -1.10$ in cumene², and $\rho^+ = -1.0$ in C₆H₅Cl¹

(12) (a) Eyring, H. *J. Chem. Phys.* **1935**, *3*, 107. (b) Absolute rate theory states that vibration/rotation of the bond being broken should be replaced by a translational mode. The translation could be also termed loose vibration/rotation. The replacement of vibration/rotation by translation can trigger increase of activation entropy. The translational motion concerns three dimensions whereas vibration and rotation occur with one and two dimensions, respectively.

(13) Refer to Supporting Information.

Table 2. Activation Parameters for Thermal Decomposition of *tert*-Butyl Phenylperacetates in CDCl₃

activation parameter	<i>p</i> -CH ₃ O	<i>p</i> -PhO	<i>p</i> -CH ₃	<i>p</i> -Ph	H	<i>p</i> -Cl	<i>m</i> -Cl	<i>p</i> -NO ₂
ΔH^\ddagger_Y ^a	27.52 ± 0.54	28.08 ± 0.53	28.24 ± 0.50	28.16 ± 0.70	26.82 ± 0.53	26.61 ± 0.58	26.08 ± 0.40	26.20 ± 0.59
ΔS^\ddagger_Y ^b	5.87 ± 1.50	5.58 ± 1.49	4.90 ± 1.41	4.37 ± 1.96	-0.92 ± 1.48	-1.84 ± 1.61	-4.83 ± 1.13	-6.39 ± 1.65
$\Delta\Delta H^\ddagger_{Y-H}$ ^{a,c}	0.70	1.26	1.42	1.33	0	-0.22	-0.73	-0.62
$\Delta\Delta S^\ddagger_{Y-H}$ ^{b,d}	6.79	6.50	5.82	5.28	0	-0.92	-3.91	-5.47
$T\Delta\Delta S^\ddagger_{Y-H}$ ^{a,e}	2.40	2.30	2.05	1.87	0	-0.33	-1.38	-1.93

^a In kcal mol⁻¹. ^b In eu. ^c $\Delta\Delta H^\ddagger_{Y-H} = \Delta H^\ddagger_Y - \Delta H^\ddagger_H$. ^d $\Delta\Delta S^\ddagger_{Y-H} = \Delta S^\ddagger_Y - \Delta S^\ddagger_H$. ^e $T = 353$ K.

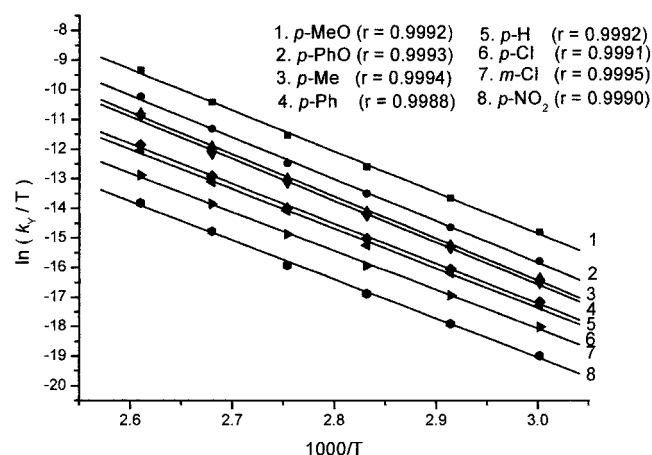
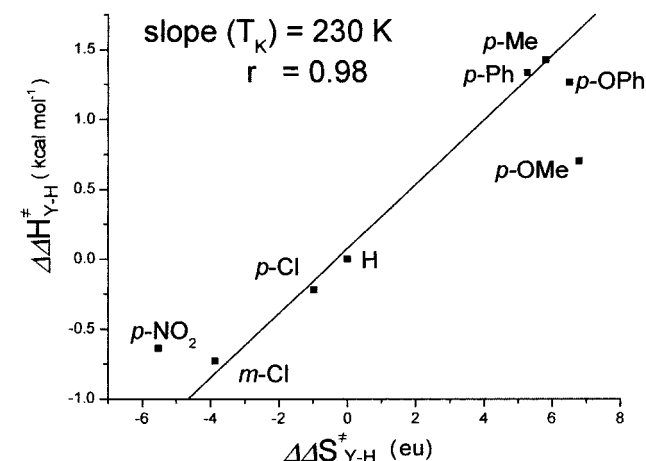
Figure 1. Eyring plot of $\ln(k_T/T)$ vs $1000/T$.

Figure 2. Isokinetic relationship by enthalpy/entropy compensation effects.

at 80 °C). The values of activation enthalpy (ΔH^\ddagger_Y) appear comparable in CDCl₃ (Table 2) and in C₆H₅Cl (Table 1 of ref 1c) despite of different solvents and unidentical methods of measurement. These similar figures (ρ^+ and ΔH^\ddagger_Y) may suggest little solvent interference with **1**. Activation parameters should thus be determined mainly by substituent interactions. Locations of bonds *y* and *z* are too far separated from the substituent for the interactions to take place. Therefore, **1** can experience quite similar substituent interactions influencing reactivities of photobrominations of substituted toluenes⁹ and cumenes¹¹ and β -scissions of the carbinyloxy radicals.¹⁰ The deviation behaviors of *p*-OCH₃, *p*-OPh, and *p*-NO₂ may suggest that the substituents engender activation processes that are, more or less, different from those triggered by the rest of the substituents.

Contribution of Activation Enthalpy. Electron donors (attractors)^{7,9-11} tend to stabilize (destabilize) the

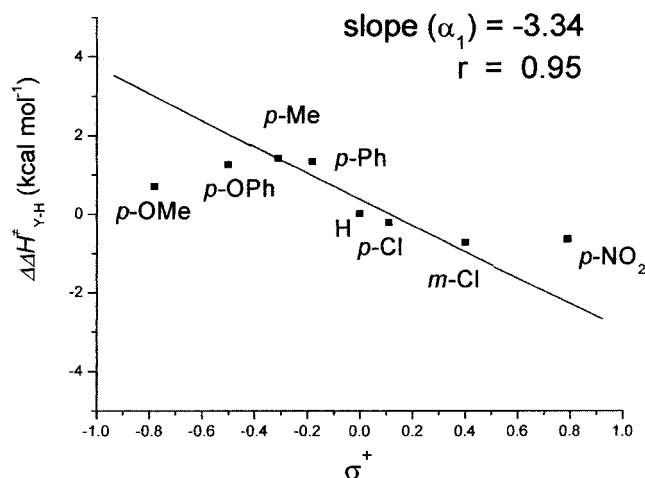


Figure 3. Perturbation of activation enthalpy by substituent effects.

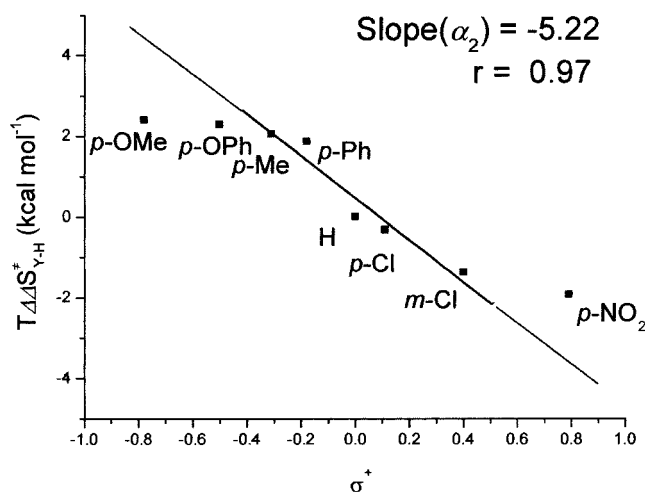


Figure 4. Perturbation of activation entropy by substituent effects.

cationic moiety of **1**, which can be mainly effected through delocalization of positive charge accompanied by formation of double bond *w* (factor *a*). Factor *a* provokes to decrease (increase) magnitude of ΔH^\ddagger_Y for the donors (attractors). The stabilization (destabilization) may then lengthen (shorten) the extent of cleavage of *x* (factor *b*). Factor *b* tends to counteract the effect of factor *a* on the magnitude of ΔH^\ddagger_Y . Cleavage of *x* occurs with C–C sigma bond that is accompanied by formation of C–C pi bond of *w*. Therefore, the donors (attractors) could render ΔH^\ddagger_Y larger (smaller) than in the case of the substituent being hydrogen atom, i.e. *Y* = H. Accordingly, *b* overwhelms *a* to determine the size of differential activation enthalpy ($\Delta\Delta H^\ddagger_{Y-H}$). The secondary α -deuterium kinetic isotope effects⁷ also suggest the pivotal role of *b* for the rates. Figure 3 shows a good linearity (slope -3.34; *r*

0.950) with five substituents ($Y = p\text{-CH}_3$, $p\text{-Ph}$, $p\text{-H}$, $p\text{-Cl}$, and $m\text{-Cl}$). Differential activation enthalpy ($\Delta\Delta H^\ddagger_{Y-H}$) could be the net change derived from the compensating effects of a and b when substituent Y replaces the hydrogen atom on the phenyl ring of **1**. $p\text{-CH}_3$ ($\Delta\Delta H^\ddagger_{Y-H} = 1.42 \text{ kcal mol}^{-1}$) and $p\text{-Ph}$ ($\Delta\Delta H^\ddagger_{Y-H} = 1.33 \text{ kcal mol}^{-1}$) exhibit $\Delta\Delta H^\ddagger_{Y-H} > 0$ because increment of ΔH^\ddagger_Y perturbed by b is larger than the reduction of ΔH^\ddagger_Y caused by a . $p\text{-Cl}$ and $m\text{-Cl}$ are the attractors and show $\Delta\Delta H^\ddagger_{Y-H} < 0$, i.e., $-0.22 \text{ kcal mol}^{-1}$ for $p\text{-Cl}$ and $-0.73 \text{ kcal mol}^{-1}$ for $m\text{-Cl}$. The negative figures can occur when a is again excelled by b during the activation. A similar switchover of the sign from $\Delta\Delta H^\ddagger_{Y-H} > 0$ to $\Delta\Delta H^\ddagger_{Y-H} < 0$ has been already observed with the photobrominations of substituted toluenes.⁹ On the other hand, activation enthalpies (ΔH^\ddagger_Y) are almost immune to substituent effects to render corresponding differential terms close to nil (i.e., $\Delta\Delta H^\ddagger_{Y-H} \approx 0$) for β -scissions of the carbinyloxy radicals¹⁰ and photobrominations of substituted cumenes.¹¹ This phenomenon^{10,11} has been rationalized in terms of the cancellation of the opposite effects invoked by a and b .

$p\text{-OCH}_3$ ($\sigma^+ -0.78$)¹⁴ and $p\text{-OPh}$ ($\sigma^+ -0.50$)¹⁴ share negative deviations with Figure 3. Both substituents can disperse positive charge on **1** into their own oxygen atoms forming a quinoid-like TS. The extra charge dispersion helps a reduce size of ΔH^\ddagger_Y yielding $\Delta\Delta H^\ddagger_{Y-H} = 0.70$ and $1.26 \text{ kcal mol}^{-1}$ for $p\text{-OCH}_3$ and $p\text{-OPh}$, respectively. Photobrominations of substituted toluenes⁹ also show a very similar negative deviation with $p\text{-OCH}_3$ carrying $\Delta\Delta H^\ddagger_{Y-H} = 0.73 \text{ kcal mol}^{-1}$. The effect of a becomes significant enough to give the negative deviation but hardly excels contribution of b for $\Delta\Delta H^\ddagger_{Y-H} > 0$. The disturbance of activation enthalpy by $p\text{-OCH}_3$ ²⁵ again reveals a positive value, i.e., $\Delta\Delta H^\ddagger_{Y-H} = 1.2 \text{ kcal mol}^{-1}$, when *tert*-butoxy radical abstracts hydrogen atom from $p\text{-CH}_3\text{OC}_6\text{H}_4\text{OH}$.

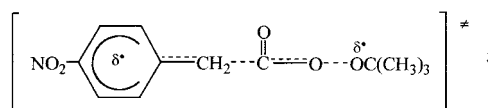
Figure 3 shows a positive deviation for $p\text{-NO}_2$. Homolysis of the perester bearing $p\text{-NO}_2$ has shown viscosity-dependent rates⁴ and exhibits very low secondary α -deuterium kinetic isotope effect (compare $k_{YH}/k_{YD} = 1.051$ for $p\text{-NO}_2$ with $k_{YH}/k_{YD} = 1.293$ for $p\text{-OCH}_3$).⁷ Furthermore, $p\text{-NO}_2$ delivers $\sigma^+ = 0.79$,¹⁴ which can drastically destabilize the cationic site of **1**. These phenomena, altogether, might have suggested that $p\text{-NO}_2$ prevents cleavage of **x** and promotes scission of **z** only. However, our activation enthalpy for $p\text{-NO}_2$ marks $\Delta H^\ddagger_Y = 26.20$

Table 3. Activation Parameters of Homolysis of Various Initiators

initiators	ΔH^\ddagger (kcal mol ⁻¹)	ΔS^\ddagger (eu)
$\text{C}_6\text{H}_5\text{C}(\text{O})\text{OOC}(\text{CH}_3)_3^a$	37.5	16.1
$(\text{CH}_3)_3\text{COOC}(\text{CH}_3)_3^b$	37.8	13.8
$\text{CH}_3\text{C}(\text{O})\text{OO}(\text{O})\text{CCH}_3^c$	31.3	11.6
$(\text{C}_6\text{H}_5)_2\text{C}=\text{C}=\text{NCH}_2\text{C}_6\text{H}_5^d$	25.4	-1.1
$\text{C}_6\text{H}_5\text{CH}_2\text{CO}_3\text{C}(\text{CH}_3)_3^e$	26.8	-0.9
$(\text{C}_6\text{H}_5)_2\text{CHCO}_3\text{C}(\text{CH}_3)_3^f$	24.3	-1.0
$\text{C}_6\text{H}_5\text{CH}=\text{CHCH}_2\text{CO}_3\text{C}(\text{CH}_3)_3^f$	23.5	-5.9

^a Ref 21. ^b Ref 22. ^c Ref 23. ^d Ref 19. ^e Table 2 of this paper. ^f Ref 1.

kcal mol⁻¹, which is far below $\Delta H^\ddagger = 37.5 \text{ kcal mol}^{-1}$ for *tert*-butyl perbenzoate undergoing one-bond homolysis (Table 3). Thermal decomposition of *tert*-butyl 1-arylcycloalkanepercarboxylates⁶ also shows characteristic values of activation enthalpy for one-bond ($\Delta H^\ddagger_Y = 34.4 \text{ kcal mol}^{-1}$) and two-bond ($\Delta H^\ddagger_Y = 27.0 \text{ kcal mol}^{-1}$) homolysis involving $p\text{-NO}_2$ (refer to Table 3 of ref 6). The photobrominations of 4-substituted 3-cyanotoluenes¹⁵ proceed through a TS assuming reduced polarity. The cyano group with $\sigma_m = 0.62$ ¹⁴ may destabilize the cationic site to yield a less polar TS that could be compensated by contribution of spin delocalizations. $p\text{-NO}_2$ is a notorious spin delocalizer¹⁶⁻¹⁹ and carries a spin delocalization constant $\sigma_C^* = 0.57$.¹⁶ The plot⁷ of k_{YH}/k_{YD} vs σ^+ also shows a remarkable positive deviation (refer to Figure 1 of ref 7). Accordingly, $p\text{-NO}_2$ may induce the concerted bond cleavages traversing homolytic TS **3**. Thermolysis of $p\text{-NO}_2$ produces three entities, i.e. $p\text{-NO}_2\text{PhCH}_2^\bullet$, CO_2 , and $(\text{CH}_3)_3\text{CO}^\bullet$. The three cage species can undergo recombination if viscosity of the solvents retards the rotational diffusion in order to keep the coplanarity mentioned by Bartlett and Hiatt.¹ The reactions of other peresters²⁰ involving **1** may not experience similar cage reactions because the electronic reorganization should be preceded. Therefore, only the rate of thermal decomposition of $p\text{-NO}_2$ involving **3** can diminish with increase of solvent viscosity.



Contribution of Activation Entropy. One-bond homolysis²¹⁻²³ reveals positive activation entropy ($\Delta S^\ddagger > 10 \text{ eu}$) with the exception of isomerizations of ketenimines¹⁹ (Table 3). The reactions of a ketenimine¹⁹ discloses $\Delta S^\ddagger_Y = -1.1 \text{ eu}$, which has been attributed to loss of degrees of freedom of the TS derived from the restricted rotations of the phenyl ring.²⁴ Other negative activation entropies due to such hindered rotations occurring in two-bond homolysis are shown in Table 3. Our values of activation entropy (ΔS^\ddagger_Y) seem to be relatively small being $\Delta S^\ddagger_Y < 10 \text{ eu}$ (Table 2). Small figures can be primarily attributed to decrease the rotational degree of freedom derived from the formation of two π bonds.

The electron donors such as $p\text{-CH}_3$ and $p\text{-Ph}$ can make a stronger π bond (w) through a and bring about reduction of rotational entropy. On the contrary, the influence of b derived from bond cleavage (x) provokes to increase the translational entropy. The positive sign of $\Delta\Delta S^\ddagger_{Y-H}$ for $p\text{-CH}_3$ (5.82 eu) and $p\text{-Ph}$ (5.28 eu) can occur when increment of translational entropy outweighs dec-

(14) March, J. *Advanced Organic Chemistry*, 4th ed.; Wiley: New York, 1992; Chapt 9.

(15) (a) Fisher, T. H.; Meierhoefer, A. W. *J. Org. Chem.* **1978**, *43*, 220 and 224. (b) Fisher, T. H.; Dershem, S. M.; Prewitt, M. L. *J. Org. Chem.* **1990**, *55*, 1040.

(16) Creary, X.; Mehrsheikh-Mohammadi, M. E.; McDonald, S. J. *Org. Chem.* **1987**, *52*, 3254.

(17) Dust, J. M.; Arnold, D. R. *J. Am. Chem. Soc.* **1983**, *105*, 1221.

(18) (a) Jiang, X.-K.; Ji, G.-Z. *J. Org. Chem.* **1992**, *57*, 6051. (b) Jiang, X.-K. *Acc. Chem. Res.* **1997**, *30*, 283.

(19) Kim, S. S.; Zhu, Y.; Lee, K. H. *J. Org. Chem.* **2000**, *65*, 2919.

(20) The TS assumes a polar structure. However, the products are neutral species, i.e., YPhCH_2^\bullet , $(\text{CH}_3)_3\text{CO}^\bullet$, and CO_2 .

(21) Blomquist, A. T.; Bernstein, I. A. *J. Am. Chem. Soc.* **1951**, *73*, 5546.

(22) Raley, J. H.; Rust, F. F.; Vaughan, W. E. *J. Am. Chem. Soc.* **1948**, *70*, 1337.

(23) Smid, J.; Rembaum, A.; Szwarc, M. *J. Am. Chem. Soc.* **1956**, *78*, 3315.

(24) The idea of negative entropy due to the restricted rotations of the phenyl ring has been kindly proposed by Professor T. T. Tidwell.

(25) (a) Das, P. K.; Encinas, M. V.; Steeken, S.; Scaiano, J. C. *J. Am. Chem. Soc.* **1981**, *103*, 4162. (b) The negative sign of activation entropies ($\Delta S^\ddagger_Y < 0$) can be understood in terms of TS structure of the hydrogen abstractions.

rement of rotational entropy. Hydrogen abstractions from substituted phenols by *tert*-butoxy radical²⁵ exhibit $\Delta S^\ddagger_Y = -5.10$ eu for *p*-OCH₃ and $\Delta S^\ddagger_Y = -11.72$ eu for *p*-H. The reaction of *p*-OCH₃ indicates the differential entropy term of $\Delta\Delta S^\ddagger_{Y-H} = 6.62$ eu, which can be again attributed to dominance of *b* against *a* when *p*-OCH₃ takes place of *p*-H. Utilizing electron-withdrawing ability, *p*-Cl and *m*-Cl may provide weaker π bond (*w*) and less bond cleavage (*x*). Therefore, the rotation could become less frozen via *a* and the translation should be curtailed by *b*. The negative differential entropy values (*p*-Cl $\Delta\Delta S^\ddagger_{Y-H} = -0.92$ eu; *m*-Cl $\Delta\Delta S^\ddagger_{Y-H} = -3.91$ eu) can be produced when *b* excels *a*. Accordingly, plot of $T\Delta\Delta S^\ddagger_{Y-H}$ vs σ^+ (Figure 4) shows a good linear relationship with *p*-CH₃, *p*-Ph, *p*-H, *p*-Cl, and *m*-Cl ($\alpha_2 = -5.22$, $r = 0.97$).

The negative deviations of *p*-OCH₃ ($\Delta\Delta S^\ddagger_{Y-H} = 6.79$ eu) and *p*-OPh ($\Delta\Delta S^\ddagger_{Y-H} = 6.50$ eu) in Figure 4 can be due to the quinoid-like TS of **1** that prohibits another free rotation. However, such further entropy reduction cannot still nullify the increase of translational entropy derived from *b*! Therefore, *p*-OCH₃ and *p*-OPh reveal $\Delta\Delta S^\ddagger_{Y-H} > 0$ to maintain entropic dominance. On the contrary, *p*-NO₂ exhibits a remarkable positive deviation with $\Delta\Delta S^\ddagger_{Y-H} = -5.47$ eu. A large negative value of activation entropy ($\Delta S^\ddagger_Y = -6.39$ eu) may also strongly support two-bond homolysis (refer to Table 3). The positive deviation could be due to more flexible TS structure. The spin delocalizations occurring in **3** may engender a weaker π bond so that the rotations can be less hindered than in case of **1**.

Feature of Entropy Control of Rates. *p*-CH₃, *p*-Ph, *H*, *p*-Cl, and *m*-Cl show good linearities as shown with Figures 2, 3, and 4. The parallelism may indicate that similar mode of substituent interactions take place in the bond cleavage (*x*) and formation (*w*) in **1**. The slope of isokinetic relation of Figure 2 indicates an isokinetic temperature ($T_K = 230$ K), which is well below present reaction temperatures, indicating entropy control of rates. The entropic change multiplied by the temperature against variations of substituents (Figure 4) retains a slope of $\alpha_2 = -5.22$. The corresponding slope for the perturbation of enthalpy indicates $\alpha_1 = -3.34$ from Figure 3. The steeper slope ($\alpha_2 = -5.22$) may again suggest that the substituents influence the rates through entropic variations. The relative rates of the five substituents either slightly increase or stay constant with higher temperatures (a sign arguing for entropy control of rates).^{9–11} Such pattern of relative rates violates reactivity/selectivity principle (RSP) and can be rationalized with eq 7. Drastic skeletal alterations of R in RCO₃C-(CH₃)₃ may engender rates of the thermolysis to be influenced by an enthalpy factor. On the contrary, the variation of substituents on the phenyl ring can cause much weaker interactions²⁶ which can be properly monitored with entropy scale only.

$$Q = \Delta\Delta S^\ddagger_{Y-H}/R - \Delta\Delta H^\ddagger_{Y-H}/RT, \text{ where } Q = \ln k_Y/k_H \quad (7)$$

Conclusion

p-CH₃, *p*-Ph, *p*-H, *p*-Cl, and *m*-Cl cooperate to reveal linear relations employing differential activation param-

eters ($\Delta\Delta H^\ddagger_{Y-H}$ and $T\Delta\Delta S^\ddagger_{Y-H}$). The linear trends can be attained when the substituents systematically control the activation process. The differential activation entropy multiplied by the temperature ($T\Delta\Delta S^\ddagger_{Y-H}$) exceeds its enthalpic mate ($\Delta\Delta H^\ddagger_{Y-H}$) to realize entropy control of rates. The differential entropy terms ($\Delta\Delta S^\ddagger_{Y-H}$) are determined by counteracting contributions of translational and rotational entropies. *p*-OCH₃ and *p*-OPh are strong electron-donators and trigger an abnormally large loss of rotational entropy to give the negative deviations. However, the rates are still influenced by entropy when *b* outweighs *a*. *p*-NO₂ is such a powerful spin-delocalizer that the concerted mechanism may alternatively choose a radical-like TS. The spin dispersions can engender a weaker π bond (less hindered rotations) in **3** to afford less negative rotational entropy, which is responsible for the positive deviations. The solvent viscosity studies for *p*-NO₂ can be consistent with two-bond homolysis. The entropy scale is sensitive enough to detect relatively weak molecular interactions involving differential activation free energy $\Delta\Delta G^\ddagger_{Y-H} < 2$ kcal mol⁻¹. Activation enthalpies (ΔH^\ddagger_Y) exhibit far larger magnitudes than their differential terms ($\Delta\Delta H^\ddagger_{Y-H}$). However, differential activation entropy terms ($\Delta\Delta S^\ddagger_{Y-H}$) display figures that are comparable to or even bigger than corresponding activation entropies (ΔS^\ddagger_Y).

Experimental Section

Materials and Methods. Substituted phenyl acetic acid, *N,N*-carbonyldiimidazole, *tert*-butyl hydroperoxide, and other reagents were purchased from the major suppliers. Liquids were distilled with center-cut collection, and solids were purified according to standard procedures.²⁷ A Varian Gemini 2000 NMR spectrometer was used for the quantitative analysis of the reaction mixtures. Identifications of the products were performed with a Shimadzu GC MS-QP505A.

Ring-substituted *tert*-butyl phenylperacetates (YC₆H₄CH₂CO₃Bu^t, Y = *p*-OCH₃, *p*-OPh, *p*-CH₃, *p*-Ph, *p*-H, *p*-Cl, and *m*-Cl)⁷ were prepared by the reactions of the corresponding phenylacetic acid, *N,N*-carbonyldiimidazole, and *tert*-butyl hydroperoxide.

***tert*-Butyl *p*-nitrophenyl peracetate (p-NO₂C₆H₄CH₂CO₃Bu^t)** was synthesized according to a previous method. All the peresters show IR stretching at 1760–1770 cm⁻¹. ¹H NMR data for the peresters (CDCl₃ with 0.03% TMS): ***p*-PhO** 7.4–6.9 (m, 9H), 3.62 (s, 2H), 1.26 (s, 9H); ***p*-Ph** 7.6–7.3 (m, 9H), 3.65 (s, 2H), 1.29 (s, 9H); ***p*-Cl** 7.3–7.2 (m, 4H), 3.62 (s, 2H), 1.27 (s, 9H); ***m*-Cl** 7.3–7.1 (m, 4H), 3.62 (s, 2H), 1.28 (s, 9H). The NMR data of other peresters not given here were already provided in the previous paper.⁷

Thermal Reactions of *tert*-Butyl Phenylperacetates. Weighed samples of a perester (50 mg), acetonitrile (7 mg, internal standard), and iodine (100–150 mg) were dissolved in CDCl₃ (5 mL). The solutions were divided into several Pyrex ampules, which were degassed and sealed by a freeze–pump–thaw method. The ampules (i.d. 4 mm, length 3 cm, 2/3 full) were immersed in a constant-temperature bath for at least 200 s for thermal equilibration. Less than 20 s were required for complete thermal equilibration, which was measured by a Copper–Constantan thermocouple. At various intervals, the tubes were removed from the bath, quenched in ice–water, and opened for NMR analysis.

The integrations of the benzylic peak of a perester at $\delta = 3.6$ –3.7 ppm and the peak of acetonitrile ($\delta = 2.0$ ppm) have been made. When integrated values of the perester and acetonitrile are designated as *I_p* and *I_s*, respectively, the following equation can be obtained: $I_p/I_s = {}^2/{}_3C/C_s$. *C* and *C_s*

(26) Inoue, Y.; Ikeda, H.; Kaneda, M.; Sumimura, T.; Everitt, S. R. L.; Wada, T. J. Am. Chem. Soc. **2000**, *122*, 406

(27) Perrin, D. D.; Armarego, W. L. F.; Perrin, D. F. *Purification of Laboratory Chemicals*, 2nd ed.; Pergamon Press: Oxford, 1980.

represent the concentrations of the perester and acetonitrile, respectively. Rate constants were then produced by the method of least squares from $\ln(C_0/C_t) = k_Y t$. C_0 and C_t are concentrations of the perester at time 0 and t , respectively. C_0 has been fixed as a concentration of a perester that already underwent homolysis for more than thermal equilibration time. Most of the plots of $\ln(C_0/C_t)$ vs t showed excellent linear relations ($r \geq 0.9990$). However, the reactions of *p*-methoxyphenyl and *p*-phenoxyphenyl peresters did not show simple first-order kinetics. The product analysis suggested that corresponding benzyl iodides are unstable under the reaction conditions, which could interfere with homolysis of the perester. Pyridine has been added to trap the benzyl iodides so as to observe first-order kinetics.

Acknowledgment. We warmly thank Korea Research Foundation (KRF) for a Non-Directed Research Fund (1996–1999). Technical assistance was provided by Mr. Ji Young Song and Miss Eun Jung Kim. We are also indebted to Brain Korea 21 provided from Ministry of Education through KRF.

Supporting Information Available: Graphical plots of $\ln C_0/C_t$ vs t have been provided to show the accurate measurement of rate constant (k_Y). This material is available free of charge via the Internet at <http://pubs.acs.org>.

JO010143J